REPORT DOCUMENTATION PAGE

Form Approved
OMB No. 0704-0188

1. REPORT DATE *(DD-MM-YYYY)*	2. REPORT TYPE	3. DATES COVERED *(From - To)*
09-30-1999	Final	Apr 1998 - 12-1998

4. TITLE AND SUBTITLE
Active/Passive Remote Sensing of the Ocean Surface at Microwave Frequencies

5a. CONTRACT NUMBER
N00014-98-1-0627

5b. GRANT NUMBER
N00014-98-1-0627

5c. PROGRAM ELEMENT NUMBER

6. AUTHOR(S)
Stephen J. Frasier

5d. PROJECT NUMBER

5e. TASK NUMBER

5f. WORK UNIT NUMBER

7. PERFORMING ORGANIZATION NAME(S) AND ADDRESS(ES)
University of Massachusetts
Elec. & Comp. Engr.
Knowles Engineering Building
Amherst, MA 01003

8. PERFORMING ORGANIZATION REPORT NUMBER

9. SPONSORING/MONITORING AGENCY NAME(S) AND ADDRESS(ES)
Office of Naval Research Regional Office Boston
495 Summer Street Room 103
Boston, MA 02210-2109

10. SPONSOR/MONITOR'S ACRONYM(S)

11. SPONSORING/MONITORING AGENCY REPORT NUMBER

12. DISTRIBUTION AVAILABILITY STATEMENT
APPROVED FOR PUBLIC RELEASE

13. SUPPLEMENTARY NOTES

14. ABSTRACT
attached

15. SUBJECT TERMS

16. SECURITY CLASSIFICATION OF:			17. LIMITATION OF ABSTRACT	18. NUMBER OF PAGES	19a. NAME OF RESPONSIBLE PERSON
a. REPORT	b. ABSTRACT	c. THIS PAGE		15	Stephen J. Frasier
					19b. TELEPONE NUMBER *(Include area code)* (413) 545-4582

FINAL REPORT:
Active/Passive Remote Sensing of the Ocean Surface at Microwave Frequencies

ONR Grant: N00014-98-1-0627

R.E. McIntosh, Principal Investigator

S.J. Frasier, Co-PI (PI, effective 7/98)

University of Massachusetts

Microwave Remote Sensing Laboratory

Amherst, MA 01003

Submitted to

Office of Naval Research

September 29, 1999

Contents

1. Introduction

This report summarizes research activities and results obtained under grant N00014-99-1-0627 "Active/Passive Remote Sensing of the Ocean Surface at Microwave Frequencies" for the period of performance April 13, 1998 to April 12, 1999. This grant supported preliminary measurements of sea surface emission obtained with a Ka-band polarimetric radiometer in combination with Doppler radar measurements to characterize the surface wave field. Measurements were completed during April 1999 by the Microwave Remote Sensing Laboratory at the University of Massachusetts.

2. Goals & Objectives

Most all published measurements of microwave polarimetric emission have been obtained from aircraft where the radiometer antenna observes a large area of the sea surface. As such, these measurements inherently average over the surface wave field, and the polarimetric brightness wind speed/direction signature is parameterized by wind only. Because of the weakness of the polarimetric signature (a few K), the effect of sea-state (e.g. wave steepness) may be significant in proper interpretation of the polarimetric signature. However, as stated, few if any measurements reveal the effects of surface waves. Under this grant, MIRSL was funded to obtain preliminary measurements of the polarimetric emission's response to surface waves.

3. Approach

Our approach was to observe emission from a small spot on the ocean surface as surface waves propagate through. An X-band Doppler scatterometer was co-located with the radiometer to measure the instantaneous wave field. The purpose was to permit cross-spectral analysis of radiometric emission measurements with radar measurements of surface wave orbital velocity, similar to numerous historical measurements of the radar Modulation Transfer Function.

An initial attempt at this measurement was performed in November 1998 near Gloucester, MA. Here, instrumentation was deployed from the roof of the Hammond Castle Museum observing relatively shallow water near the shoreline. This deployment was largely unsuccessful due to inclement weather and equipment malfunctions. Measurements were repeated in April 1999 at another location in Buzzards Bay. The remainder of this report discusses these measurements.

4. Work Completed: Summary of Activities

4.1 Experimental Setup

MIRSL deployed the Ka-band Polarimetric Radiometer (KAPR) operating at 36 GHz from the seaward end of a small research pier located at the UMass Center for Marine Science & Technology (CMAST) in New Bedford, MA. The pier extends approximately 50 m into Clark's Cove adjacent to New Bedford harbor (see figure 1). Water depth at the end of pier is approximately 3 m, and tide modulation is typically less than 1 m at this location. Fetch is limited to about 16 km by the Elizabeth Islands to the South and Southeast.

The radiometer was placed on a rotatable mount located on the corner of the pier as indicated in figure 2. During this deployment it was possible to observe emission at 3 incidence angles, 45°, 55°, and 65°, and at four azimuth angles spanning 90° in 30° increments (the azimuth scan range can be improved to over 150° in the future).

An X-band Doppler scatterometer was deployed simultaneously with the radiometer to measure the instantaneous wave field. The purpose of this was to permit cross-spectral analysis of radiometric measurements with Doppler measurements of surface wave orbital velocity, as has been done in numerous radar measurements of the radar Modulation Transfer Function [1]. The radar employed a pair of standard gain horns that were mounted on the radiometer housing radiometer and boresighted with the radiometer antenna. The in-phase and quadrature channels from the radar were digitized on two unused radiometer recording channels. The data acquisition system was configured to sample at 256 Hz to satisfy the Nyquist requirements for the radar while the integration time for the radiometer channels was set to 10 ms. A video camera was also mounted on the structure to obtain a visual record of the footprint, and a meteorological station was erected measuring wind speed (U_{10} approximately), wind direction, temperature, and pressure. During this deployment, the FOPAIR-II radar was also deployed for engineering tests but could not observe the same area as the radiometer due to obstruction by the shed.

The radiometer was operated in a Dicke switching mode and was calibrated using atmospheric tip curves for a cold calibration source and observation of an ambient load (microwave absorber) for a warm source. During this experiment we were able to measure the first 3 Stokes parameters, T_H, T_V, and U, by using a switching ferrite polarization switch at the throat of the horn antenna. In one state, the radiometer measures T_H and T_V, while in the other, it measures T_{+45} and T_{-45}.

Figure 1: The UMass Center for Marine Science & Technology (CMAST) is located near Clark's Point (star) near the mouth of Clark's Cove and across Buzzard's Bay from Woods Hole.

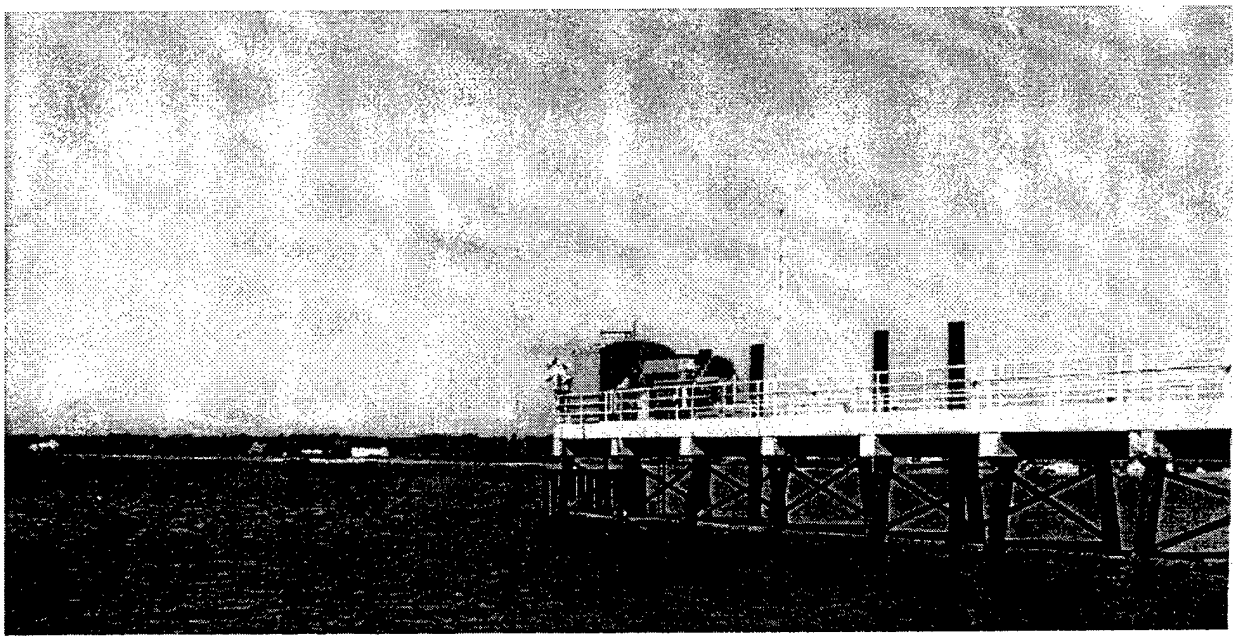

Figure 2: Photo of experimental setup on CMAST pier. The radiometer/scatterometer/video are visible at the end of the pier. The anemometer is mounted atop the tower. The FOPAIR radar is located between the tower and the shed.

The third Stokes parameter, U, can be obtained from the difference of the 45° rotated channels,

$$U = 2Re < E_V E_H^* > \approx T_{+45} - T_{-45}. \quad (1)$$

The radiometer was switched between $T_{H,V}$ and $T_{\pm 45}$ modes at 30 second intervals.

During the deployment we performed two types of measurements: Scans and Time-series. For scans, we observed each of 4 azimuth angles for each of the 3 incidence angles (12 positions total). Dwell time at each position was limited to 2 minutes to allow an entire scan in a reasonable amount of time during which environmental conditions could be assumed constant. This provided 1 minute of observation for each mode of the radiometer. While too short for stable surface wave statistics, this duration is sufficient to observe trends with incidence and azimuth angle.

For time-series, we observed a single incidence and scan angle for 17 minutes. Again, we switched between radiometer modes at 30 second intervals. Each 30 s segment is sufficiently long to get good frequency resolution of the surface wave spectra (0.033 Hz), and 17 such spectra can be averaged over the observation time for each polarization.

5. Summary of Results

5.1 Scan

Figure 3 shows results of a scan performed on May 7, 1999 for the T_H and T_V channels. Wind speed was approximately 7 m/s from 30° azimuth. Shown are the observed brightness temperatures for horizontal (left) and vertical (right) polarizations as a function of incidence angle (top) and azimuth angle (bottom). In all cases, the trends appear consistent with reported measurements and predictions. T_H decreases with incidence angle, while T_V increases. A weak azimuthal modulation is evident showing a decrease in T_V off the wind angle and a corresponding increase in T_H. Absolute temperatures for T_V are quite consistent with model predictions in [2], while T_H appears a bit warm and a bit less sensitive to incidence angle than expected. [1] From [2], it was not clear what, if any, correction for sky temperature was applied. We have not taken out the reflected sky component here. From tip curves immediately prior to this scan, estimated sky temperatures were approximately 19K for zenith (1 atm) and 36K at 60° zenith (2 atm).

[1] We have observed some, as yet unexplained, behavior in the near-zenith angle looks for the tip curves. These may have been corrupted by contributions from the shed or from an equipment winch at the end of the pier. Unfortunately, these call in to question the absolute accuracy of brightness temperatures (within a few K) reported here.

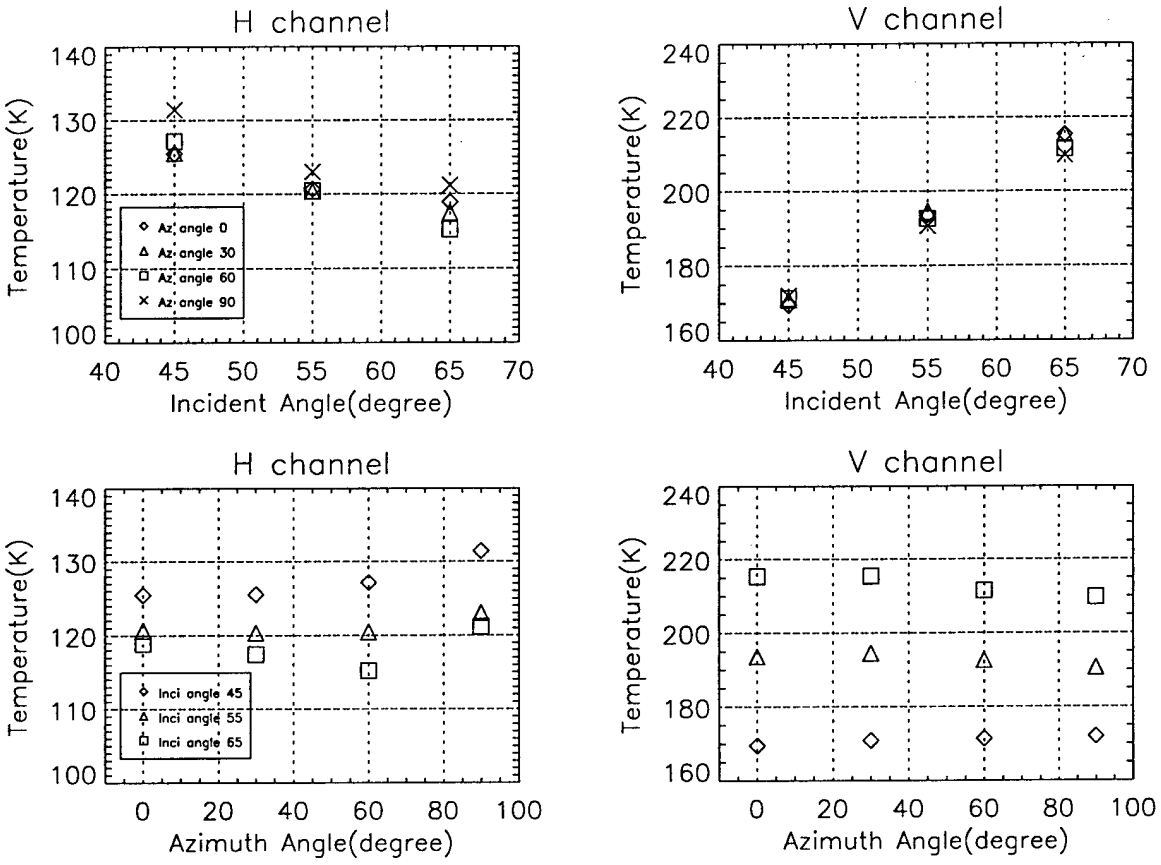

Figure 3: Horizontally polarized (left) and vertically polarized (right) brightness temperatures vs. incidence angle (top) and azimuth angle (bottom). Winds were approximately 7 m/s from 30°.

Figure 4 shows the data obtained at 65° incidence and 30° azimuth (upwind). The top two traces show T_{+45} and T_{-45} during the first and third 30 s segments and T_H and T_V during the second and fourth segments. The third trace shows $U = T_{+45} - T_{-45}$ during the appropriate segments. The lower two traces show the backscatter and Doppler velocity time-series from the radar. Here we can see that $T_{+45} \approx T_{-45} \approx 165$K, which is the average of T_H and T_V as it should be, since

$$T_{\pm 45} = \frac{1}{2}(T_H + T_V \pm U) \tag{2}$$

In theory, the mean value of U should be zero upwind (upwave), which we don't observe exactly. This is likely due to shortcomings of the calibration. The modulation on the brightness temperature signals is O(5K).

As we scan off the wind direction, we see an interesting effect in the $T_{\pm 45}$ channels (figure 5). To the left of the wind direction, we see T_{+45}'s sensitivity to the waves increase while T_{-45}'s decreases, and to the right of the wind direction, the opposite happens. There is also a suprisingly large signal swing on these channels off the wind direction. This may be a consequence of the short, relatively steep gravity waves (see next section). Since U is the mean value of the difference of these signals, it appears that the asymmetry of the wave field introduces a "bias" in the mean of the wave-sensitive channel. This is relatively easy to observe here since U is an odd function of angle with respect to the wind. In the limit of a flat sea (no wind, or very young seas) we should expect no difference between left and right of upwind. This data appears to imply that the steepness of the waves plays a role in defining the magnitude of the U (and conceivably V) signals. Since developing seas tend to have steeper waves than fully developed seas, this might be an observable characteristic in a more comprehensive data set. The T_H and T_V sensitivities to the wave field are less observable here, as they are even functions of wind aspect angle.

Finally, though the instantaneous brightness temperatures have variances that appear quite large, measurements by an airborne or spaceborne sensor average over *many* ocean wavelengths. The variances of these measurements will be quite small, provided conditions are reasonably uniform over the footprint. We can equate our 30 second data segments to "equivalent footprints" through the phase velocity of the dominant waves. The phase velocity of a 2.5 s period wave is nearly 4 m/s, so the distance traveled in 30 s is 120 m.

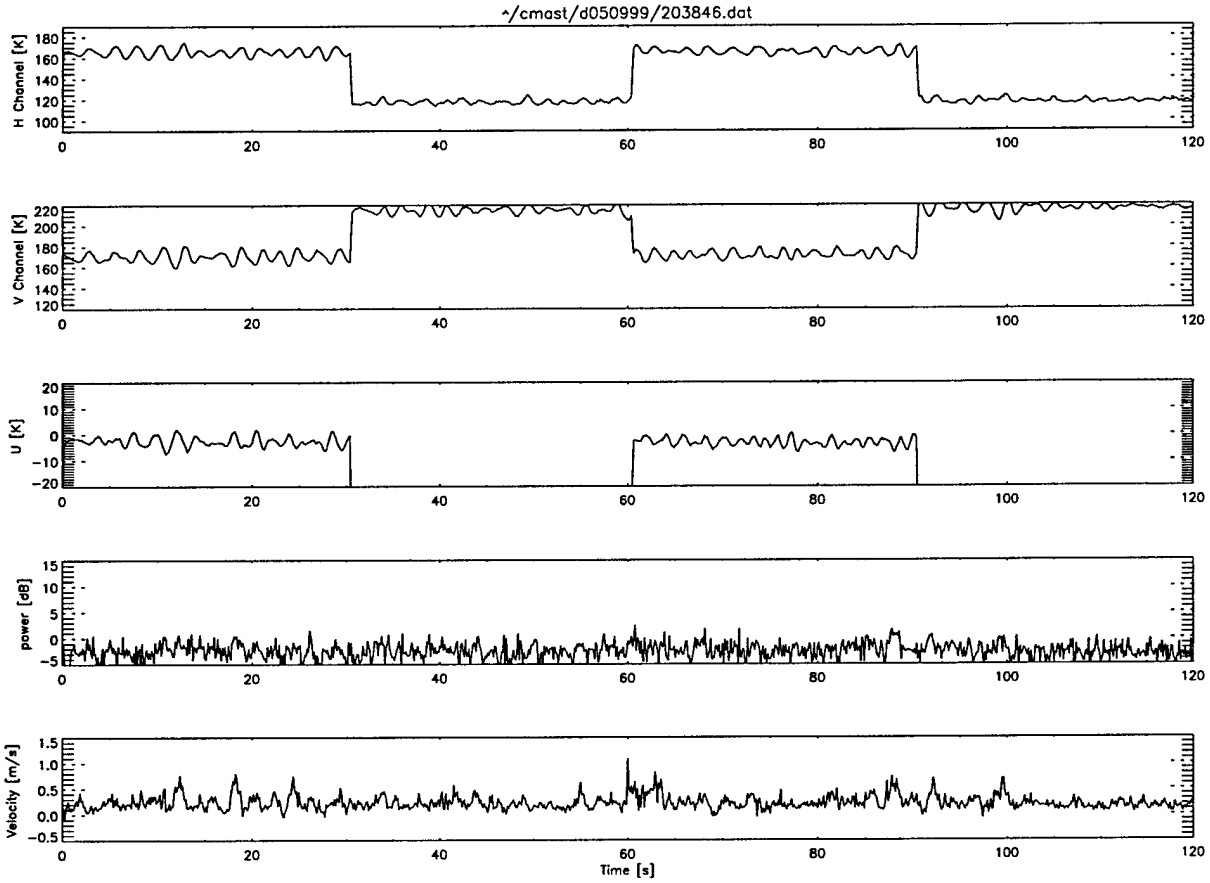

Figure 4: Two minute record at $\theta = 65°$, upwind. In the upper two traces, the first and third data segments are T_{+45} (H channel) and T_{-45} (V channel); second and fourth segments are T_H and T_V. Third trace is U, lower two traces are radar backscatter and Doppler.

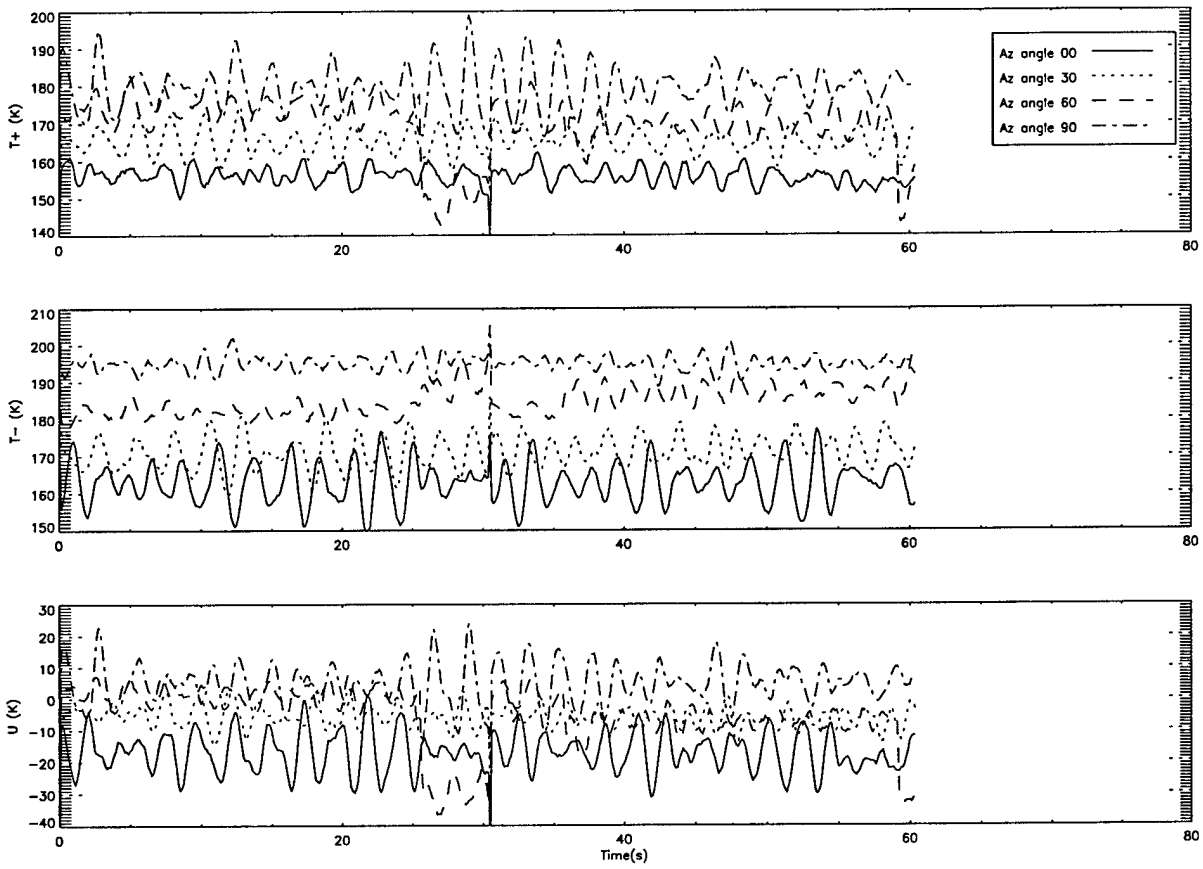

Figure 5: T_{+45}, T_{-45}, U **at** $\theta = 65°$ **for four azimuth angles. For display purposes, traces are offset in increments of 10K as follows:** $0°$ **– -10K;** $30°$ **– 0K (upwind);** $60°$ **– +10K,** $90°$ **– +20K.**

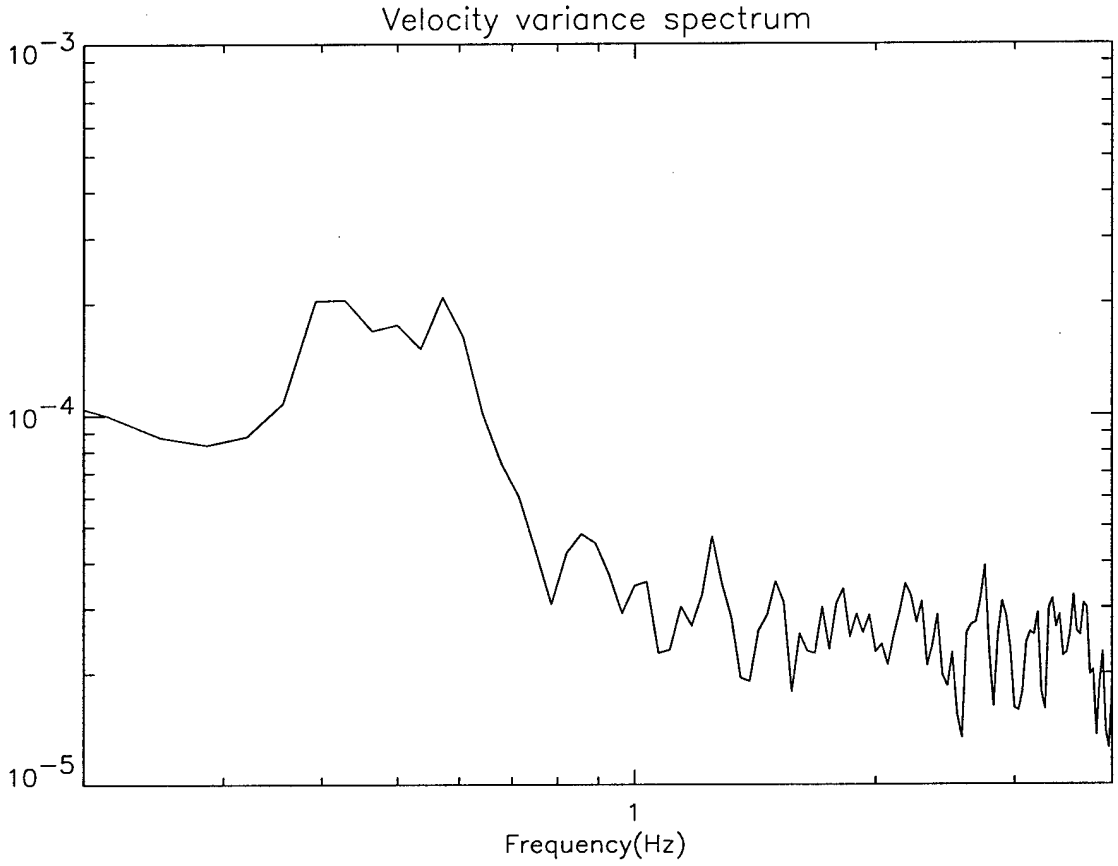

Figure 6: Surface wave orbital velocity spectrum from the radar

5.2 Time-series

Figure 6 shows the orbital velocity spectrum of the wave field for the data in this report. This was calculated using a 17 minute record. Estimated rms orbital velocity is $v_{rms} = 40$ cm/s, and the dominant wave period is $T \approx 2.5$ s. From these, one may obtain rms height as $h_{rms} = 16$ cm. The corresponding dominant wavelength is $\Lambda = 10$ m and rms slope, $s_{rms} = 6°$. These are approximate values as effect of finite water depth has been neglected here (though $\tanh(Kd) \geq 0.9$). Thus, the waves are relatively short and a somewhat steep which may account for the large wave-induced variations in brightness temperatures. Winds were 6-7 m/s.

Figure 7 shows computed coherences and relative phase angles between brightness temperature signals and the orbital velocity. These indicate good correlations at wind-wave frequencies as expected. The relative phases have not been corrected for radar incidence angle, so they are with

respect to maxima in line-of-sight velocity ($\theta = 55°$) which occurs forward of the advancing wave crest.

We find that T_H appears correlated with surface waves over a wider range of frequencies than T_V. We find that the difference in phase angles of T_H and T_V is not 180° as we might expect from models (and from our elevation scans) indicating opposite dependences on incidence angle. It appears closer to 90° from this data. We do not have an explanation for this as yet. The $T_{\pm 45}$ correlations are lower and do not peak in the same places, though the statistics are still a bit noisy after averaging 17 spectra. The phase angles of these two signals are more or less the same.

6. Impact & Applications

To our knowledge, these preliminary observations of high-resolution polarimetric emission from the sea surface have not been reported elsewhere. In particular, the ability to observe the response of the $T_{\pm 45}$ channels to the surface waves has provided useful and intuitive insight into the origin of the directional signal of U. Correlation with a radar-derived wave record allows us to determine the response of the Stokes parameters to the instantaneous wave field. Some of our observations appear inconsistent with expectations and should be studied further. It would also be useful to obtain more complete statistics on the magnitude of the azimuthal modulations in T_H, T_V, and U as functions of wave steepness (rms slope) or wave age.

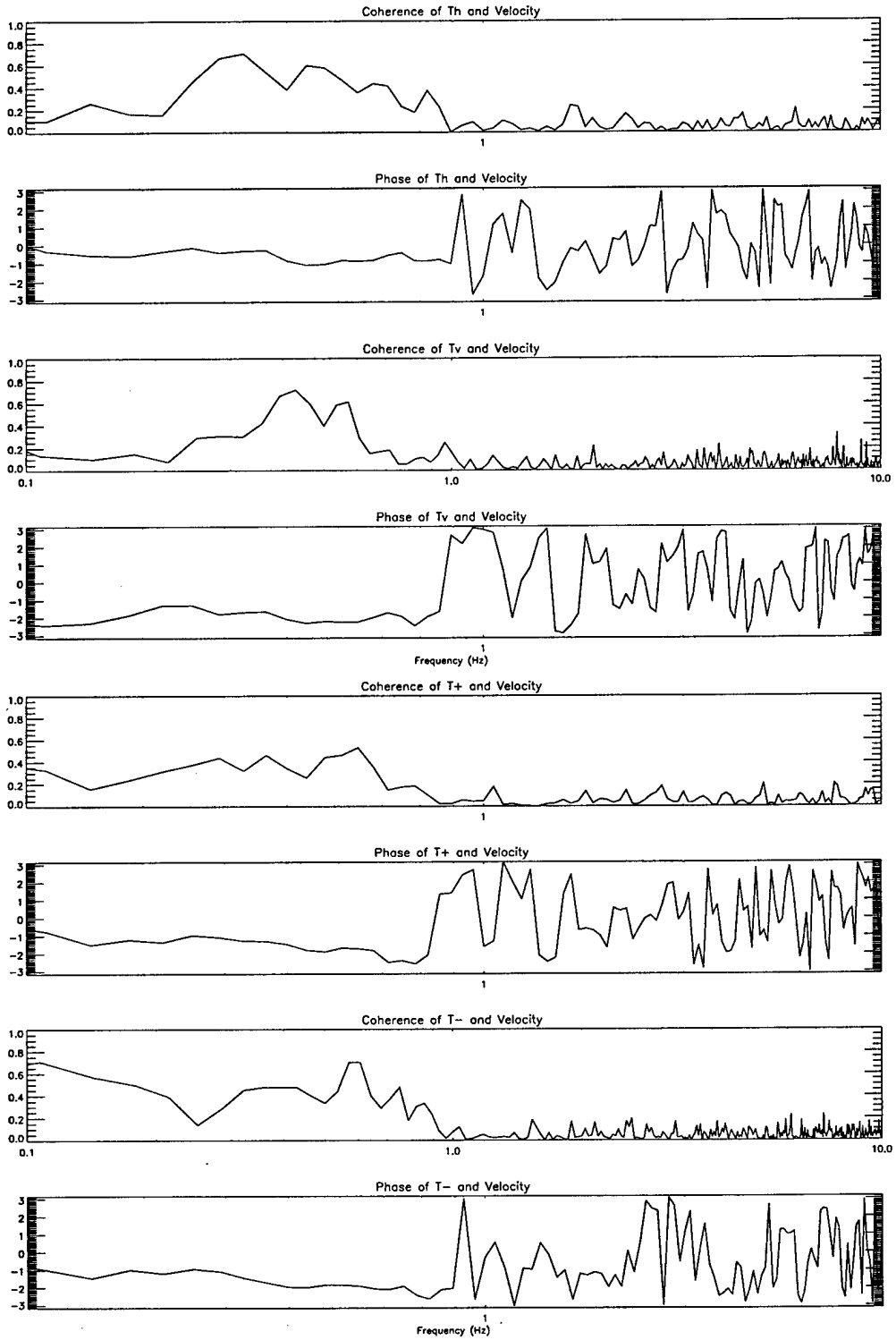

Figure 7: Coherences and relative phases between brightness temperatures and line-of-sight orbital velocity. Upwind, $\theta = 55°$.

7. Summary of Publications

1. Wang, F., S.J. Frasier, E.J. Knapp, J.R. Carswell, C.T. Swift, "Preliminary Observations of Polarimetric Sea Surface Emission Measured from a Pier", submitted to *2000 National Radio Science Meeting*, Boulder, CO, Jan 3–7, 2000.

8. Other Statistical Information

1. Number of graduate students supported: 2

References

[1] W.J. Plant, ", in *Radar Scattering from Modulated Wind Waves*, K.J. Komen and W.A. Oost, Eds., chapter The Modulation Transfer Function: Concept and Applications, pp. 155–172. Kluwer Academic Publishers, 1989.

[2] S.H. Yueh, "Modeling of wind direction signals in polarimetric sea surface brightness temperatures", *IEEE Transaction on Geoscience and Remote Sensing*, vol. 35, no. 6, pp. 1400–1417, 1997.